

## Silicon carbide cluster entrapped in a diamond from Fuxian, China

IRENE S. LEUNG

Department of Geology and Geography, Lehman College, City University of New York, Bronx, New York 10468, U.S.A.

### ABSTRACT

An inclusion found in a diamond from Fuxian contains four blue-green,  $6H$  SiC crystals, overgrown by apparently younger, colorless grains of the  $3C$  polytype. Structures of both polytypes are well ordered. This multicrystalline cluster is surrounded by a thin layer of K-Al-Si-rich glass in which an extremely Fe-rich spherule is embedded. Many minute rhombs of calcium carbonate and two prismatic calcium sulfate crystals occur in the glass. Observations were made petrographically, by SEM, and by single-crystal X-ray techniques.

In addition to being unique owing to its unusual mineral association, the inclusion is bounded by uncommon curved surfaces. This paper presents the first detailed account of mantle-derived SiC extracted from a natural diamond and reports the first appearance of calcium sulfate and a rare occurrence of calcium carbonate as diamond inclusions, although it is not possible to determine if both of the latter crystallized while the diamond host resided in the mantle. The absence of macroscopic glass inclusions in diamond may be due to subsequent crystallization of trapped melt, if any. Finally, there is little doubt that cubic SiC is an as-yet unnamed legitimate mineral species.

### INTRODUCTION

A diamond from Fuxian in Liaoning Province contains three inclusions of SiC crystals. The largest is a polymorphic cluster of four hexagonal ( $\alpha$ -SiC) and numerous cubic ( $\beta$ -SiC) crystals, all encrusted with colorless and brown glass. Set in the glass matrix are crystallites of two Ca-bearing minerals. The inclusion assemblage is an uncontaminated specimen derived from the source region where the diamond host crystallized. This paper describes distinctive characteristics of this unusual inclusion.

The existence of SiC as a natural mineral has been in dispute for at least 50 years. In a study of the Canyon Diablo iron meteorite, Moissan (1904) reported finding SiC as green, hexagonal crystals but noted that it also occurred in the form of fragments (Moissan, 1905). The hexagonal form of SiC was given the name moissanite by Kunz (1905). As this mineral has never been identified by subsequent researchers of the same meteorite, the source of Moissan's SiC might have been introduced during cutting of the meteorite (Mason, 1967). Many geologists are greatly concerned that most SiC grains reportedly found in various rock types are, in reality, fragments of carborundum used in grinding rocks (Milton and Vitaliano, 1985). In this paper, the chemical formula, SiC, is used instead of the mineral name, moissanite, which refers only to the hexagonal form, whereas no mineral name has been proposed for the cubic form.

In a study of mineral inclusions in diamond occurring in lamproite from Western Australia, Jaques et al. (1989) reported finding one crystal of SiC, briefly described as having an X-ray pattern corresponding very closely to the  $6H$  polytype. Inclusions of SiC in diamonds were report-

edly found also in kimberlites from the Monastery mine in South Africa (Moore and Gurney, 1989) and the Sloan diatremes in North America (Otter and Gurney, 1989). SiC has been reported as an accessory mineral in diamond-bearing kimberlites in the Mir and Aikhal pipes of the Siberian Platform (Bobrievich et al., 1957; Marshintsev et al., 1967), and the Mengyin pipes of Shandong, China (He, 1984, 1987). All of these Asian samples are reported to be  $\alpha$ -SiC. Crystals of  $\alpha$ -SiC found in volcanic breccia in a region of kimberlitic rocks in Bohemia (Bauer et al., 1963) may also have a close affinity to, and possibly originated in, kimberlite itself. The first reported natural occurrence of  $\beta$ -SiC was in shale of the Green River Formation in Wyoming, where it was proposed to have formed by means of hot fluids that originated in volcanic activity (Regis and Sand, 1958). It is difficult to assess the true identity of this  $\beta$ -SiC for lack of sufficient analytical data in the report. The second occurrence of  $\beta$ -SiC was reported as small, black spherules included in  $\alpha$ -SiC crystals in kimberlitic rocks (Marshintsev et al., 1982), and its identification was based on an X-ray powder diffraction pattern. It is unlikely that tiny black spherules could be separated completely from the  $\alpha$ -SiC host during preparation of the X-ray sample. Therefore, as X-ray lines of  $\beta$ -SiC and the host  $\alpha$ -SiC (type  $15R$ ) almost completely overlap, the presence of  $\beta$ -SiC could not have been recognized without resorting to single-crystal X-ray diffraction under those circumstances. In a study of submicrometer-sized residues separated by acid treatment of the Murray carbonaceous chondrites, Bernatowicz et al. (1987) identified  $\beta$ -SiC based on high resolution lattice imaging and interplanar spacings and angles measured on electron diffraction patterns. Recently, we discovered

macrocrystals of  $\alpha$ -SiC overgrown epitaxially by  $\beta$ -SiC in kimberlites from Fuxian (Leung et al., 1990).

### DIAMOND FROM FUXIAN

SiC was reported by He (1984) as a minor component in kimberlites occurring in Shandong, but no detailed descriptions of this mineral can be found in the Chinese literature. Other geologists in China confirmed that SiC is a common accessory mineral in most kimberlites in China, and because of the mineral's close association with diamond, it is reportedly used to locate diamond prospects (Zhang and Chen, 1978). I traveled to Shandong and Liaoning in 1986 and 1987, respectively, to acquire inclusion-bearing diamonds and specimens of SiC still in the kimberlite matrix.

The sample used in this research is a cluster of SiC crystals encapsulated in an octahedral diamond 1.3 mm in size (Fig. 1A) obtained from the Fuxian diamond mine, located approximately 90 km north of the port city of Dalian in Liaoning. Kimberlite pipes, located at the intersection of two secondary fault systems, about 40 km east of the deep north northeast-trending Tanlu Fault, penetrated Proterozoic sandstone overlain by Paleozoic sediments (Hu et al., 1986). Since only Pipe 50 was being excavated at the mine during 1987, the SiC-bearing diamond purchased at the processing plant at Pulandian is, therefore, most likely a product of Pipe 50.

### EXPERIMENTAL TECHNIQUES

The SiC-bearing diamond is free of fractures in the immediate vicinity of its largest inclusion, but two other small SiC crystals (110  $\mu\text{m}$  and 80  $\mu\text{m}$ , respectively, in their longest dimension) are located at internal tension cracks (Fig. 1A). After the diamond was broken mechanically, only the largest inclusion was recovered. It is about 180  $\mu\text{m}$  in its longest dimension and was found to be a multicrystalline assemblage during a petrographic examination. After a photograph was taken under incident, fiber-optic light (Fig. 1B), the inclusion was attached to a gelatine slide, immersed in a drop of oil to increase transparency, and then photographed again using both incident and transmitted plane-polarized light (Fig. 1C). After removal of the inclusion from the slide, thin shells of colorless and brown material, appearing isotropic between crossed polarizers, were found in the gelatine. These shells, subsequently identified as glass, shattered at the tip of a needle used in an attempt to retrieve them.

Detailed morphological and chemical studies of the crystalline and glass phases were made using a JSM-U3 scanning electron microscope (SEM) equipped with an

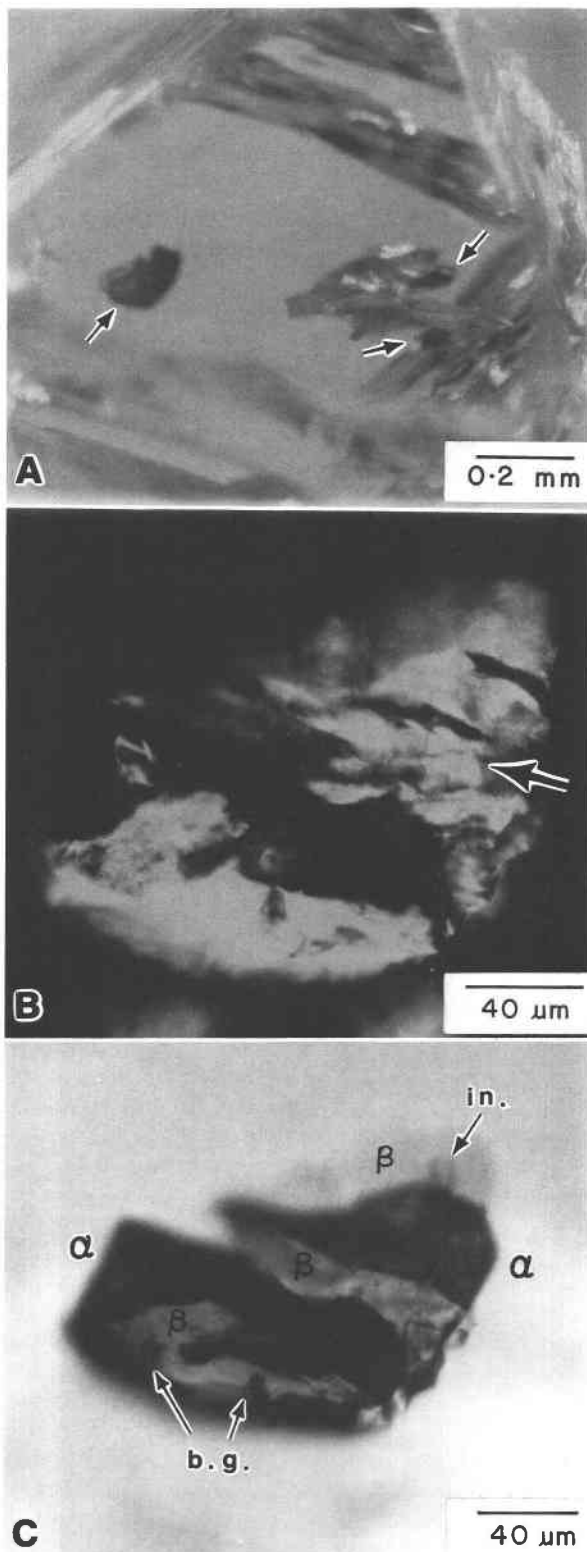


Fig. 1. Photomicrographs of (A) diamond from Fuxian containing three separate inclusions of SiC, indicated by arrows. (B) Cluster of SiC crystals extracted from diamond, viewed under incident light. Dark = blue-green  $\alpha$ -SiC; white and gray = colorless  $\beta$ -SiC; arrow indicates region with granular texture. (C)

Same specimen immersed in oil, seen in transmitted light. Dark rectangular  $\alpha$ -SiC crystal is partly overgrown by colorless  $\beta$ -SiC (lower half of specimen); dark irregularly shaped (drumstick-shaped) area consists of three individual  $\alpha$ -SiC crystals; gray =  $\beta$ -SiC; b.g. = brown glass; in. = inclusion.

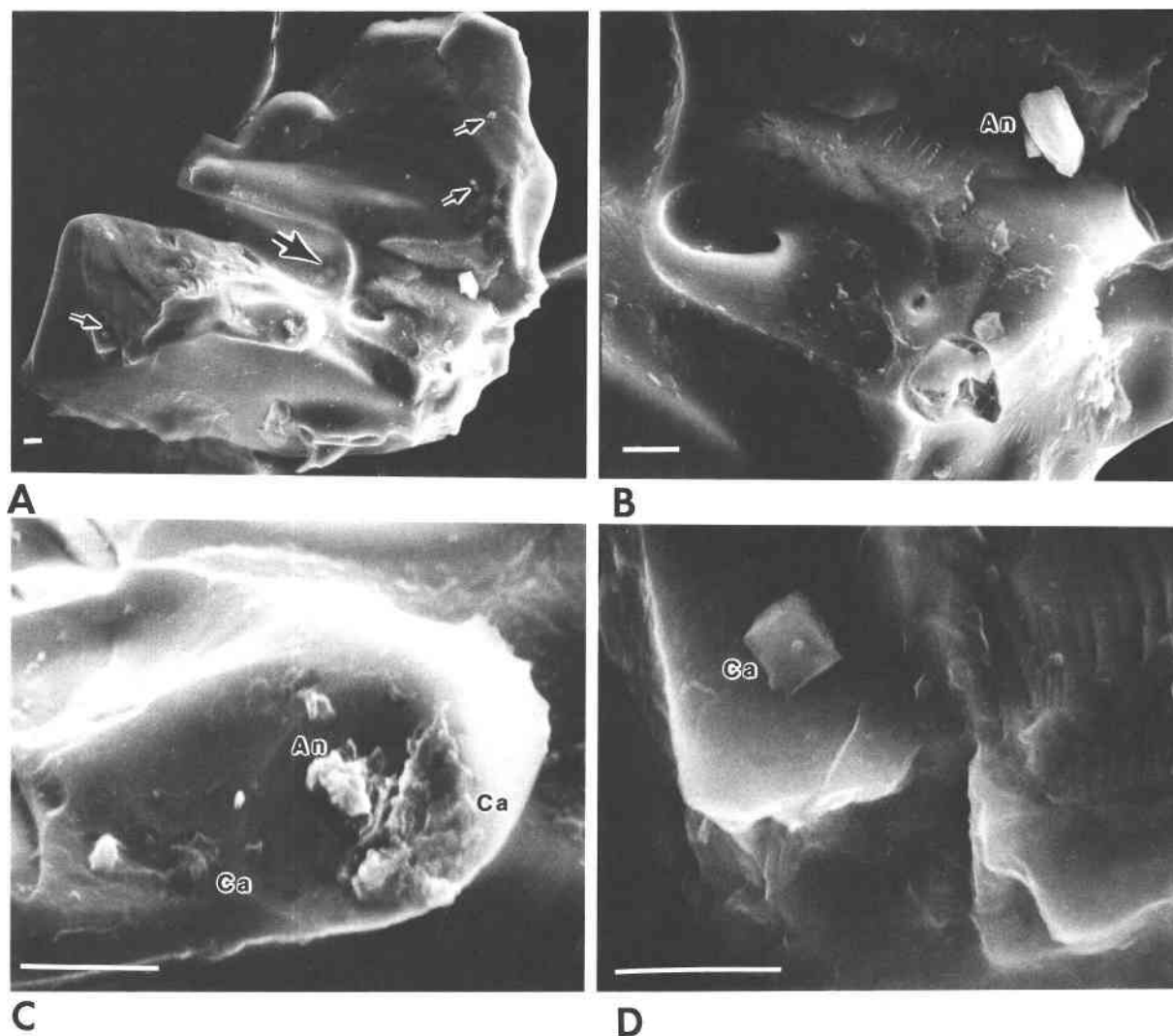


Fig. 2. SEM images showing (A) curvatures of glass-rimmed SiC cluster. Big arrow indicates Fe-rich spherule; small arrows point at rhombs of calcium carbonate. (B) Two prismatic calcium sulfate crystals (An) on surface of SiC. (C) Prismatic crystallites of calcium sulfate (An); aggregates of calcium carbonate (Ca). (D) Rhombohedral crystal of calcium carbonate (Ca); conchoidal fractures in SiC (upper right). All scale bars = 5  $\mu\text{m}$ .

energy-dispersive X-ray (EDX) spectrometer. Because SiC is a fairly good electrical conductor, no C coating of the sample was necessary. The inclusion assemblage was further examined in an Amray 1830 SEM mounted with a PGT Si(Li) windowless detector to verify the presence of C in both SiC and carbonate crystals. Identifications of minute crystalline phases other than SiC are solely based on their EDX spectra and morphologies. In all EDX analyses, a beam energy of 20 keV was necessary to provide adequate overvoltage to excite X-ray lines. Counting time was 100 s, except for a very Fe-rich spherule for which it was increased to 300 s.

A powder X-ray diffraction pattern obtained from the inclusion assemblage using a 57.3 mm Gandolfi camera shows severe darkening of the film background due to

scattering of X-rays by a significant amount of glass encrusting the inclusion, which caused weak diffraction lines derived from minute crystallites to be undetectable. Finally, the inclusion was transferred to a single-crystal precession camera to record data of individual crystals existing within the SiC cluster. Extraneous reflections on each reciprocal-lattice net are accounted for by finding orientations of small domains to which they belong. Exposures of each X-ray precession photograph required 6–8 d.

## RESULTS

The inclusion extracted from the Fuxian diamond is a complex cluster of SiC crystals coated with colorless and brown glass to which many Ca-bearing crystallites ad-

here. Identified crystalline and glass phases are reported below, followed by a description of SiC polytypes existing in the sample and their structural relationships.

### Crystalline phases

Major identified crystalline phases forming the bulk of the inclusion are four  $\alpha$ -SiC and numerous  $\beta$ -SiC crystals. Crystals of blue-green  $\alpha$ -SiC appear black in Figure 1C, where the large crystal ( $140 \times 50 \mu\text{m}$ ) is approximately rectangular in shape, although it is partly overlapped by colorless  $\beta$ -SiC. The irregularly shaped black area toward the upper portion of Figure 1C consists of three individual  $\alpha$ -SiC crystals identified by single-crystal diffraction techniques. A layer  $25 \mu\text{m}$  thick of  $\beta$ -SiC (Fig. 1C, uppermost area of  $\beta$ -SiC) also consists of three cubic crystals distinguishable only by X-ray diffraction. Included in the same area are eight unidentified, micrometer-sized grains displaying very high birefringence between crossed polarizers, the largest of which can be seen in Figure 1C, whereas many others are out of focus. Colorless  $\beta$ -SiC may appear as continuous overgrowths, and its granular texture is more prominent in some areas than others (see Fig. 1B). Although both polytypes are rimmed by a veneer of glass, EDX spectra of SiC can occasionally be obtained from glass-free areas. Such spectra show the presence of only two major chemical elements, Si and C, and a very small amount of Al.

Minor crystalline phases include many isolated rhombs and crystalline masses of calcium carbonate (Figs. 2A, 2C, and 2D), and two idiomorphic crystals (Fig. 2B) and many aggregates (Fig. 2C) of calcium sulfate. The large calcium sulfate crystal shown in Figure 2B is over  $9 \mu\text{m}$  in length. Identifications of these Ca-bearing phases are solely based on their EDX spectra. EDX analyses of very small carbonate crystals include spectra not only from an individual crystal, but also from its veneer of glass and the underlying SiC crystal, resulting in composite spectra such as that reproduced as Figure 3A. X-ray peaks appearing in Figure 3A are derived from three phases: magnesian calcium carbonate, SiC, and K-Al-Si glass. Compared with a spectrum derived from only SiC and glass (Fig. 4A), the additional height of the C peak appearing in Figure 3A is attributable to the carbonate phase. The spectrum of a much larger calcium sulfate crystal (Fig. 3B) shows only significant peaks of Ca, S, and O, with very small Si and C peaks derived from the SiC "background." All minor crystalline phases must be firmly attached to the inclusion, because they were not removed when the sample was treated in an ultrasonic cleaner.

### Glass phases

The SiC cluster is almost entirely coated with glass, except one end of the large rectangular  $\alpha$ -SiC crystal (Fig. 1C, left margin) and where conchoidal fractures are prominent (e.g., Fig. 2D, upper right). It is likely that when the diamond was broken in order to free its inclusions, parts of the glass rim (and  $\beta$ -SiC overgrowth) were accidentally ripped from the surface of the inclusion, re-

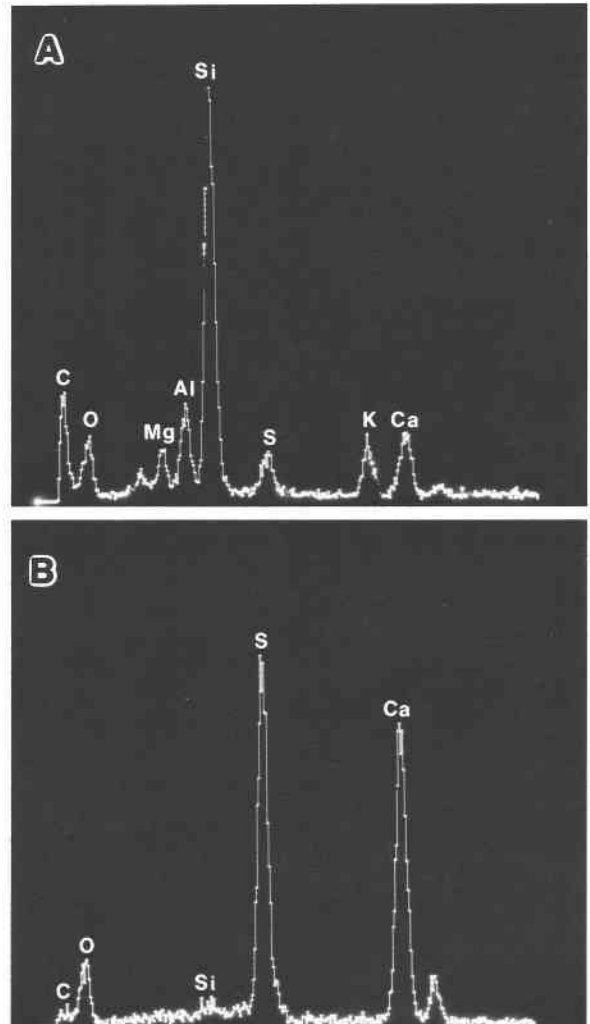
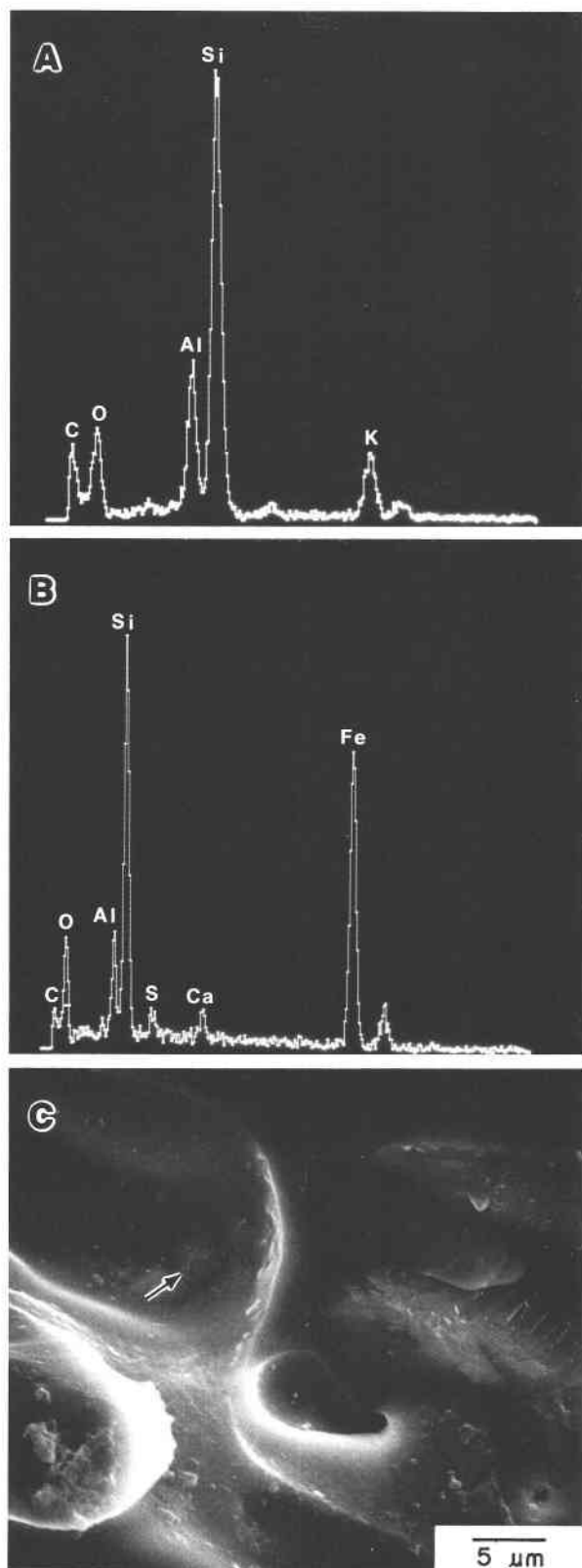


Fig. 3. EDX spectrum of (A) magnesian calcium carbonate (with K, Al, Si, O and C contributed by SiC and glass; S peak derived from mounting medium); (B) calcium sulfate. 20 keV (0–5 keV), counting time = 100 s.

sulting in glass-free areas. Small areas covered with brown glass are visible under a petrographic microscope (Fig. 1C). Areas covered with colorless glass were discovered only when colorless areas enriched in K, Al, and Si, as determined by EDX analysis, were found to be amorphous; when these areas were X-rayed in quest of a K-Al silicate mineral, no reflections of such minerals as kalsilite, leucite, sanidine, or any other mineral were detected. A very diffuse powder diffraction pattern obtained from the inclusion assemblage by means of a Gandolfi camera has a severely darkened background because of the scattering of X-ray by an appreciable amount of glass, and only a few broadened X-ray lines of SiC can be seen.

X-ray element maps illustrate the extent of surface exposure of SiC (Fig. 5A, white areas) and areas covered with K-Al-Si glass (Figs. 5B and 5C, white areas). The sketch in Figure 5 delineates the inclusion's surface mor-



phology. Figure 4A is a typical EDX spectrum derived from the colorless glass and its underlying SiC crystal. Major elements attributable to the colorless glass are K, Al, Si and O. Areas covered with brown glass show similar spectra, which sometimes contain small peaks at the position for  $FeK\alpha$ , but since the peaks are not of statistically significant height above background, they cannot be relied upon. There is, however, an unusually Fe-rich spherical body measuring  $4\ \mu\text{m}$  in diameter (Fig. 4C, indicated by arrow) whose spectrum (Fig. 4B) also contains peaks contributed by the underlying SiC and a veneer of K-Al-Si glass. Interpretation of this spectrum will be considered below, in the discussion section.

#### Polymorphs (polytypes) of SiC

Symmetries of the SiC crystals were determined by recording reciprocal lattices of small domains of each crystal on X-ray precession photographs. Final results show that all recorded X-ray reflections are attributable to polymorphs of SiC existing within the cluster. All hexagonal and trigonal polytypes are known as  $\alpha$ -SiC, whereas cubic SiC was designated  $\beta$ -SiC by Thibault (1944) because its crystal structure is analogous to that of  $\beta$ -ZnS (sphalerite).

$\alpha$ -SiC. Four  $\alpha$ -SiC crystals have been identified. The structures of the largest rectangular  $\alpha$ -SiC crystal and the narrow end of the irregularly shaped area of  $\alpha$ -SiC (see Fig. 1C) are oriented parallel to each other, having a maximum misalignment of only  $0.6^\circ$ . Both of these crystals are elongated in the  $c$ -axis direction. The thick end of the irregularly shaped area of  $\alpha$ -SiC is composed of two randomly oriented individuals. Figure 6A is a typical zero-level  $a$ -axis precession photograph of  $\alpha$ -SiC (rectangular crystal) depicting a  $6H$  structure that is well ordered, as there is no streaking in the  $c^*$  direction between sharp diffraction spots. This phenomenon is rarely observed in synthetic SiC (Shinozaki and Kinsman, 1978). Unit-cell dimensions of  $\alpha$ -SiC as determined using precession photographs are  $a = 3.077 \pm 0.003\ \text{\AA}$ , and  $c = 15.09 \pm 0.01\ \text{\AA}$ , comparable to those of commercial SiC (Thibault, 1944). The space group of  $\alpha$ -SiC in the inclusion is  $P6_3mc$ . Additional discrete spots between the  $6H$  diffraction maxima, as observed along the  $10\bar{1}l$  lattice row, are derived from small domains of a  $4H$  polytype (e.g., Fig. 6A, reflection indicated by the large arrow).

Appearing in the  $c$ -axis precession photograph taken from the thick end of the irregularly shaped  $\alpha$ -SiC area (Fig. 6B) are extraneous reflections belonging to two cubic  $\beta$ -SiC crystals. One of the latter (two of its reflections are

←

Fig. 4. EDX spectrum of (A) colorless glass and underlying SiC. Elements in glass are K, Al, Si, and O. (B) Fe-rich spherule shown in C (with contributions from SiC, glass, and S from mounting medium). See text for interpretation of spectrum. 20 keV (0–5 keV for A, 0–10 keV for B), counting time = 100 s for A, 300 s for B. (C) SEM image showing location of Fe-rich spherule, indicated by arrow here and in Figure 2A.

indexed) was reoriented to obtain  $[1\bar{1}2]$ ,  $[001]$ , and  $[110]$  photographs (Figs. 7A–7C), and the other was adjusted to give rise to a  $[1\bar{1}2]$  photograph (Fig. 6C) in which  $[\bar{1}11]$  was horizontal. When the  $[\bar{1}11]$  axis was rotated  $90^\circ$  from its position in Figure 6C, an  $a$ -axis pattern of  $\alpha$ -SiC appeared, superimposed on a cubic  $\beta$ -SiC  $[110]$  pattern (Fig. 6D), indicating epitaxial growth in which  $(111)_\beta \parallel (0001)_\alpha$ , and  $[110]_\beta \parallel [10\bar{1}0]_\alpha$ . The photograph shown in Figure 6D also contains additional  $4H$  reflections. Unit-cell dimensions of this  $\alpha$ -SiC crystal are  $a = 3.082 \pm 0.003 \text{ \AA}$ , and  $c = 15.12 \pm 0.01 \text{ \AA}$ , identical, within experimental error, to those measured by Taylor and Laidler (1950). However, the  $c$  value is greater than that of the large rectangular crystal by about  $0.03 \text{ \AA}$ . The fourth  $\alpha$ -SiC crystal, in contrast, bears no epitaxial relation with its neighbors. Its  $[2\bar{1}\bar{1}6]$  diffraction pattern (Fig. 7D) deviates by about  $4^\circ$  from the  $[110]$  pattern of  $\beta$ -SiC (Fig. 7C).

**$\beta$ -SiC.** Three colorless  $\beta$ -SiC crystals have been identified in a layer  $25 \mu\text{m}$  thick (Fig. 1C, uppermost area of  $\beta$ -SiC). Their space group is  $F43m$ , and  $a = 4.358 \pm 0.004 \text{ \AA}$ , in good agreement with the magnitude of  $a$  of synthetic  $\beta$ -SiC made by Taylor and Laidler (1950). As already described, one of the  $\beta$ -SiC crystals is epitaxially related to  $\alpha$ -SiC. The second  $\beta$ -SiC crystal, as a result of having  $[110]_\beta \parallel [10\bar{1}0]_\alpha$ , displays abnormally intense 220 reflections as seen in the  $[001]$  photograph (Fig. 7B). A third  $\beta$ -SiC crystal, whose  $a$ -axis is designated  $a'$  in Figure 7B, shows no obvious crystallographic relationship with any other crystalline phase.

## DISCUSSION

The inclusion found in the diamond from Fuxian is composed of a unique assemblage of minerals and glass phases of unusual morphology. Polymineralic inclusions in diamond are relatively rare (Meyer, 1982), and glass, occurring with crystalline inclusions or independently, has never been reported.

### Origin of SiC

Solid inclusions, commonly bounded by planar surfaces parallel to the  $\{111\}$  and  $\{100\}$  planes of diamond, frequently appear in well-formed or distorted cuboctahedral habits regardless of their own crystal symmetry. Such negative crystals are considered cogenetic with their diamond host (Harris and Gurney, 1979). On the other hand, any mineral inclusion whose morphology reflects its own symmetry is considered to have formed before its entrapment (Meyer, 1987). The few planar surfaces observed on SiC crystals in the cluster (others may be concealed below overgrowths having curved surfaces) and the  $c$ -axis elongation observed on two  $\alpha$ -SiC crystals indicate formation before entrapment, which is further evidenced by the lack of cubic symmetry imposed on the inclusion by the diamond host.

The grain size of  $\beta$ -SiC is much smaller than that of  $\alpha$ -SiC. One of the  $\beta$ -SiC crystals is epitaxially intergrown with  $\alpha$ -SiC, as described above and indicated by Figure 6D, such that closest-packed planes of each are in common. As this  $\beta$ -SiC grain is an individual crystal having

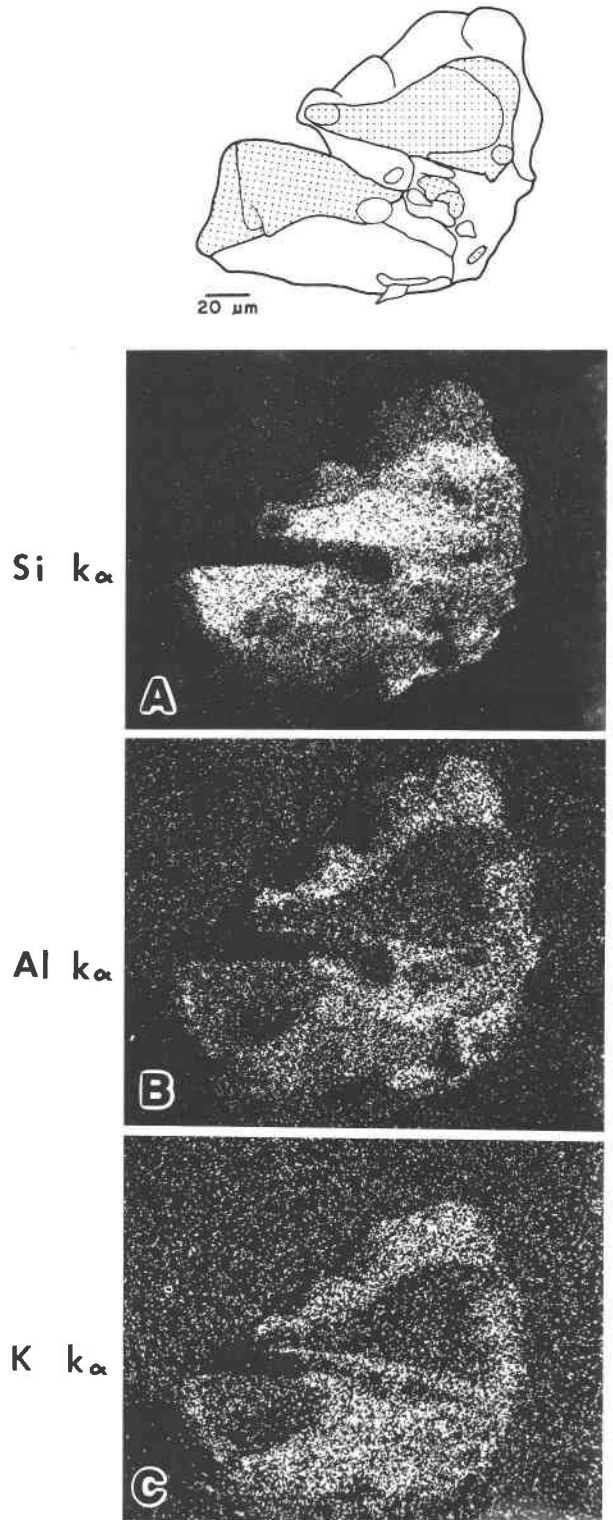


Fig. 5. X-ray element "maps" of SiC cluster showing distribution of (A)  $\text{SiK}\alpha$ ; (B)  $\text{AlK}\alpha$ ; (C)  $\text{KK}\alpha$ . Sketch shows general morphology and areas where SiC is exposed (dotted), and where covered by glass (clear areas).

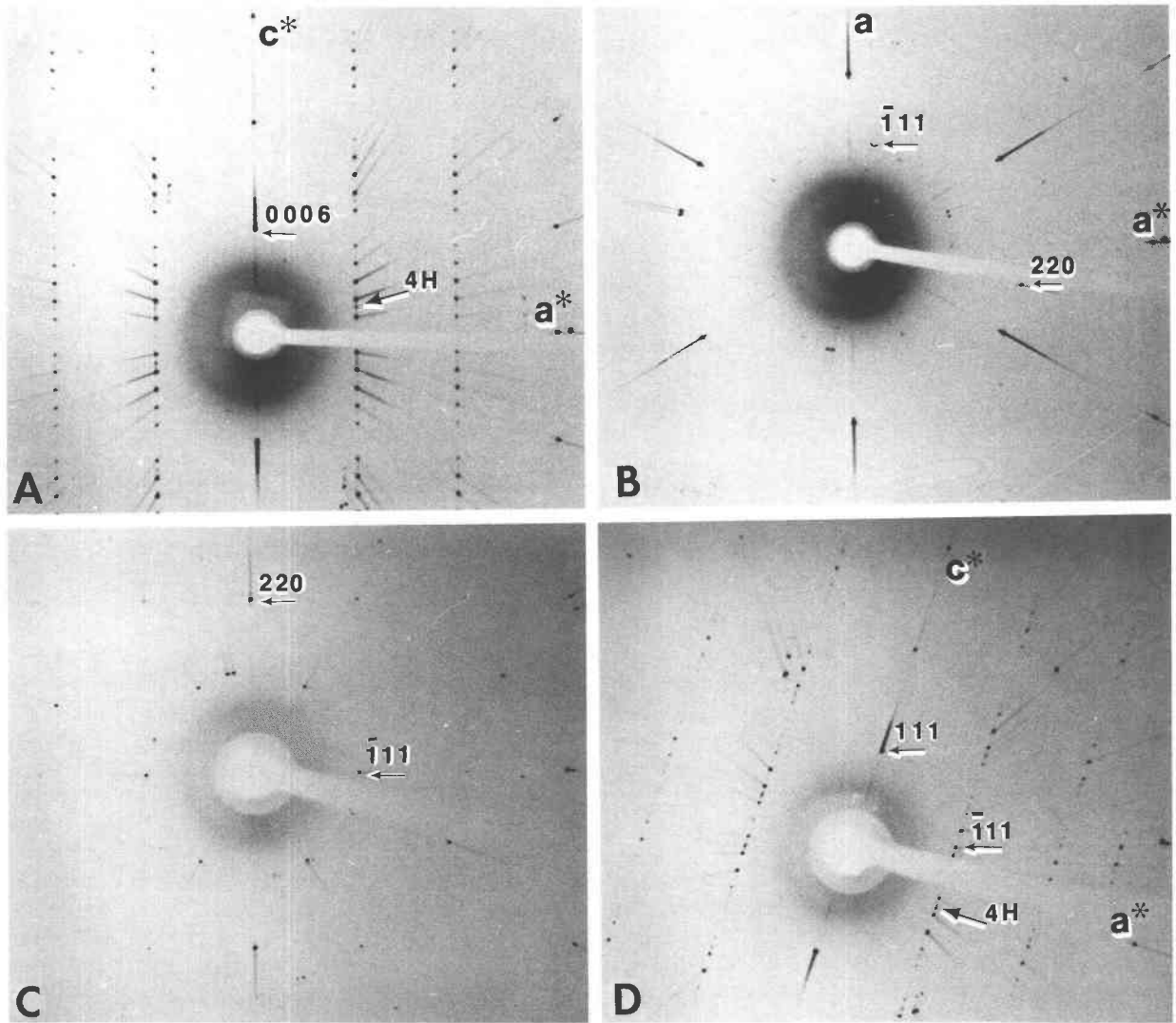


Fig. 6. X-ray precession photographs of (A)  $\alpha$ -SiC,  $a$ -axis, zero level; (B)  $\alpha$ -SiC,  $c$ -axis, zero level. Indexed extraneous reflections belong to a  $\beta$ -SiC crystal whose reciprocal lattices are shown in Figures 7A–7C. Other extraneous reflections belong to another  $\beta$ -SiC crystal adjusted to give rise to (C) [112] photograph, and (D) [110] photograph, on which an  $a$ -axis pattern of  $\alpha$ -SiC is superposed epitaxially. For all photographs: MoK $\alpha$ , 45 kV, 20 mA, exposure times = 6–8 d.

a well-ordered  $3C$  structure (Fig. 6C), the X-ray photograph shown in Figure 6D is, therefore, not a result of syntaxy (mixture of intervals of  $6H$  and  $3C$ ) nor multiple twins on (111), the latter being prevalent in synthetic SiC (Kohn and Eckart, 1962; Bootsma et al., 1971; Sato and Shinozaki, 1974). A second  $\beta$ -SiC crystal (Fig. 7B) is only slightly misoriented with respect to  $\alpha$ -SiC, whereas a third is randomly oriented (Fig. 7B,  $a$ -axis is designated  $a'$ ) and apparently developed independently. These three crystals are located in the only area through which the X-ray beam can penetrate unobstructed by  $\alpha$ -SiC (Fig. 1C, uppermost area of  $\beta$ -SiC). The number of crystals of  $\beta$ -SiC existing elsewhere cannot be determined optically or by X-rays. The SiC cluster can therefore be described as composed of four large, blue-green  $\alpha$ -SiC crystals surrounded by

granular, colorless  $\beta$ -SiC. On the basis of their spatial relationships, the two polymorphs apparently represent two generations of growth, in which  $\alpha$ -SiC is the early-formed phase, whereas the overgrowth of  $\beta$ -SiC crystallized later in time, either before or after entrapment.

#### Origin of glass and minor crystalline phases

The colorless glass shell surrounding the SiC cluster is a potassic, aluminous, silicate material. Several spots covered with brown glass show similar compositions, according to their EDX spectra, although minor additional elements that may be present in thin films of brown glass overlying a substrate of colorless glass would be difficult to detect. Be that as it may, differences in color may imply differences in chemistry. A single Fe-rich spherule

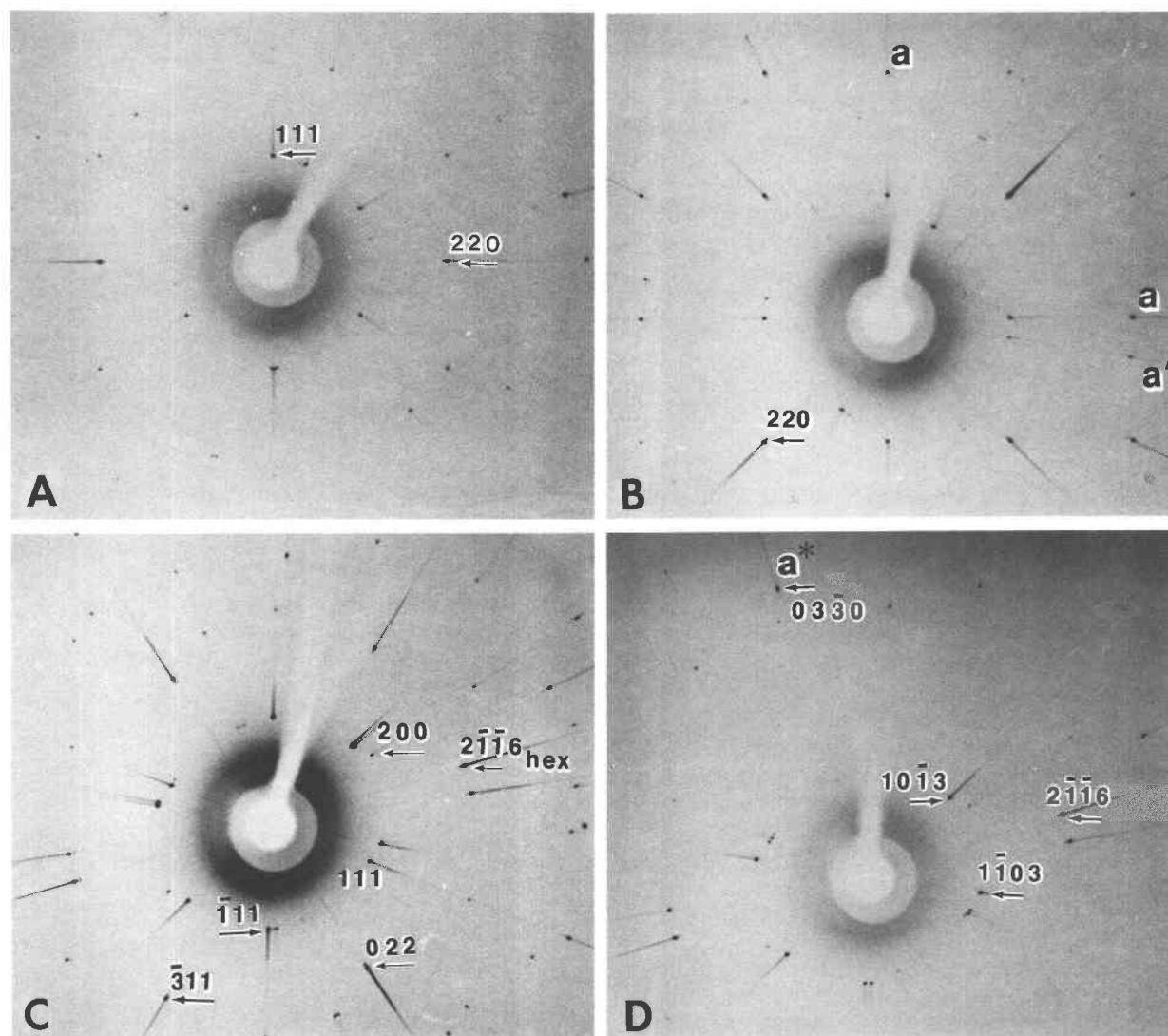


Fig. 7. X-ray precession photographs of  $\beta$ -SiC derived from indexed reflections appearing in Figure 6B. (A)  $[1\bar{1}2]$  photograph; (B)  $[001]$  photograph in which the  $a$ -axis of another  $\beta$ -SiC crystal is designated  $a'$ , and abnormally intense 220 reflections are due to  $[110]_{\beta} \parallel [10\bar{1}0]_{\alpha}$ ; (C)  $[110]$  photograph containing extraneous  $\alpha$ -SiC reflections; (D)  $[2\bar{1}\bar{1}6]$  photograph of  $\alpha$ -SiC derived from extraneous reflections appearing in C. For all photographs: MoK $\alpha$ , 45 kV, 20 mA, exposure times = 6–8 d.

(Fig. 4C) was found in an area of  $\beta$ -SiC coated with glass, and both the  $\beta$ -SiC and the glass likely contributed to the EDX spectrum of the spherule (Fig. 4B). If the peaks corresponding to the SiC and glass (Fig. 4A) are subtracted from the spectrum in Figure 4B, the resultant spectrum appears to have only one significant peak at the Fe position, representing fluorescence from only the spherule. The composition so derived would approach that of metallic Fe. Alternatively, if the peaks owing to the K-Al-Si glass are retained, then, the spherule would show a K-Al-Si-Fe composition, that of an Fe-rich melt. The time and space of origin of these glasses is unresolved.

Closely related to the K-Al-Si glass are magnesian calcium carbonate and calcium sulfate crystals resembling phenocrysts in a glassy matrix. Had the carbonate formed

while the diamond was in the mantle, then it would be classified as a primary mantle phase. On the other hand, if the carbonate crystallized during or after the kimberlite eruption, it would be designated secondary. Mantle-derived carbonates are rare, with the exception of small carbonate inclusions in megacrysts of pyrope found by McGetchin and Besancon (1973), but the crystal morphology of the carbonate was not described in their report. In diamonds containing submicrometer inclusions, infrared absorption bands characteristic of calcite have been reported (Navon et al., 1988). Calcium sulfate found in this inclusion is a new solid inclusion in diamond reported here for the first time. It is not possible to prove if this sulfate was a stable phase in the mantle or a product of secondary growth at lower temperature and pres-



sure. Similarly, another sulfate phase, barite, was found included in a Cr-bearing diopside in a South African kimberlite (Hervig and Smith, 1981), and its genesis was also unresolved.

### Characteristics and significance of natural SiC

In mining practices, resin-bonded SiC grinding discs are often used in preparing surfaces of borehole casing lengths before they are welded together (W. Jarvis, personal communication, 1990). The millimeter-sized crystals (carborundum) bonded in heavy-duty polishing paper are euhedral to subhedral rather than in the form of conchoidal fragments, as in abrasives used in making thin sections. For this reason, crystal morphology is not a good criterion for distinguishing natural SiC from carborundum. The appearance of  $\alpha$ -SiC is quite elusive because of its dark, almost opaque, color. Natural modes of occurrence of  $\beta$ -SiC have not been established, as documentations of its characteristics are lacking. According to Verma and Krishna (1966), all polytypes, except *2H* and  $\beta$ -SiC, occur in commercial SiC produced by annealing the primary reaction product,  $\beta$ -SiC, until it is totally transformed to  $\alpha$ -SiC at about 1600 °C (Ogbuji et al., 1981). This information and results derived from the present investigation suggest that the presence of  $\beta$ -SiC and well-ordered polytype structures are important characteristics distinguishing natural SiC from carborundum.

The appearance of SiC included in natural diamond provides evidence that SiC may be an important C-bearing mineral in the earth's mantle, in addition to graphite, diamond and carbonates. According to the estimate of He and Zhao (1986), the source of the Fuxian kimberlite in which the SiC inclusion may have crystallized may be deeper than 250 km. This environment, as indicated by the presence of SiC, may have an  $f_{O_2}$  value far below all estimates using other redox indicators (Woermann and Rosenhauer, 1985). Such physical and chemical conditions would control the concentrations of highly reduced minerals like SiC, but their existence would not be known unless they are tapped by deep fractures and transported rapidly to the surface before oxidation and alteration could take place. A potentially important further study of the SiC cluster would involve investigation of the C-isotope ratios of both the SiC and its host diamond. Results of such research might provide information on the C cycle, particularly with regard to sources of C, isotopic fractionation processes, presence or absence of biogenic C or recycling by subduction, and whether methane is an important gas species in the mantle.

### CONCLUSIONS

The entrapment of SiC in the Fuxian diamond is not an accidental occurrence, since SiC-bearing diamonds have reportedly been found in three other localities. The uniqueness of the Fuxian occurrence lies in the coexistence of two SiC polymorphs and their association with carbonate, sulfate, and two or three varieties of glasses. This investigation confirmed the existence of  $\alpha$ -SiC in

nature and established  $\beta$ -SiC as a legitimate mineral species.

### ACKNOWLEDGMENTS

Acquisition of rough diamond suitable for this research was arranged by Li Yau Luen and Li Xuan. Helpful discussions and communications were provided by Gene Ulmer, Irving Friedman, and Wenxiang Guo. I thank Michael Zolensky, Eric Essene, and Donald Peacor for reviewing this paper, leading to much improvement. I am solely responsible for the content of this paper. This work was supported by a grant from the Research Corporation for the purchase of an X-ray generator, and by grant no. 664159 from the PSC-CUNY Award Program of the City University of New York.

### REFERENCES CITED

- Bauer, J., Fiala, J., and Hřichová, R. (1963) Natural  $\alpha$ -silicon carbide. *American Mineralogist*, 48, 620–634.
- Bernatowicz, R., Fraundorf, G., Ming, T., Anders, E., Wopenka, B., Zinner, E., and Fraundorf, P. (1987) Evidence for interstellar SiC in the Murray carbonaceous meteorite. *Nature*, 330, 728–730.
- Bobrovich, A.P., Kalyuzhnyi, V.A., and Smirnov, G.I. (1957) Moissanite in kimberlites of the East Siberian Platform. *Doklady Akademii Nauk SSSR*, 115, 1189–1192 (in Russian).
- Bootsma, G.A., Knippenberg, W.F., and Verspui, G. (1971) Phase transformations, habit changes and crystal growth in SiC. *Journal of Crystal Growth*, 8, 341–353.
- Harris, J.W., and Gurney, J.J. (1979) Inclusions in diamond. In J.E. Field, Ed., *The properties of diamond*, p. 555–591. Academic Press, London.
- He, G. (1984) Kimberlites in China and their major components: A discussion on the physico-chemical properties of the upper mantle. In J. Kornprobst, Ed., *Kimberlites, I. Kimberlites and related rocks*, p. 181–194. Elsevier, Amsterdam.
- (1987) Mantle xenoliths from kimberlites in China. In P.H. Nixon, Ed., *Mantle xenoliths*, p. 181–185. Wiley, New York.
- He, G., and Zhao, Y. (1986) Geochemistry of porphyritic kimberlites in Mengyin County, Shandong Province, and in Fuxian County, Liaoning Province, China. In *Fourth International Kimberlite Conference, Perth, Extended Abstracts*, Geological Society of Australia Abstracts Number 16, p. 36–38.
- Hervig, R.L., and Smith, J.V. (1981) Dolomite-apatite inclusion in chrome-diopside crystal, Bellsbank kimberlites, South Africa. *American Mineralogist*, 66, 346–349.
- Hu, S., Zhang, P., and Wan, G. (1986) A review of the geology of some kimberlites in China. In *Fourth International Kimberlite Conference, Perth, Extended Abstracts*, Geological Society of Australia Abstracts Number 16, p. 121–123.
- Jaques, A.L., Hall, A.E., Sheraton, J.W., Smith, C.B., Sun, S.S., Drew, R.M., Foudoulis, C., and Ellingsen, K. (1989) Composition of crystalline inclusions and C-isotope composition of Argyle and Ellendale diamonds. In J. Ross, A.L. Jaques, J. Ferguson, D.H. Green, S.Y. O'Reilly, R.V. Danchin, and A.J.A. Janse, Eds., *Kimberlites and related rocks*, 2, p. 966–989. Blackwell Scientific, Cambridge, England.
- Kohn, J.A., and Eckart, D.W. (1962) A twinning study of cubic ( $\beta$ ) silicon carbide. *American Mineralogist*, 47, 1005–1010.
- Kunz, G.F. (1905) Moissanite, a natural silicon carbide. *American Journal of Science*, 19, 396–397.
- Leung, I., Guo, W., Freidman, I., and Gleason, J. (1990) Natural occurrence of silicon carbide in a diamondiferous kimberlite from Fuxian. *Nature*, 346, 352–354.
- Marshintsev, V.K., Shchelchkova, S.G., Zol'nikov, G.V., and Voskresenskaya, V.B. (1967) New data on moissanite from the Yakutian kimberlites. *Geologiya Geofizika Novosibirsk*, 12, 22–31 (in Russian).
- Marshintsev, V.K., Zayakina, N.V., and Leskova, N.V. (1982) New find of cubic silicon carbide, an inclusion in moissanite from kimberlitic rocks. *Doklady Akademii Nauk SSSR*, 262, 204–206 (English translation).
- Mason, B. (1967) Extraterrestrial mineralogy. *American Mineralogist*, 52, 307–325.
- McGetchin, T.R., and Besancon, J.R. (1973) Carbonate inclusions in

- mantle-derived pyropes. *Earth and Planetary Science Letters*, 18, 408–410.
- Meyer, H.O.A. (1982) Mineral inclusions in natural diamond. In D.M. Eash, Ed., *International Gemological Symposium Proceedings*, p. 445–465. Gemological Institute of America, Santa Monica.
- (1987) Inclusions in diamond. In P.H. Nixon, Ed., *Mantle xenoliths*, p. 501–522. Wiley, New York.
- Milton, C., and Vitaliano, D.B. (1985) Moissanite SiC, a geological aberration. *Geological Society of America, Abstracts with Program*, 17, 665.
- Moissan, H. (1904) Nouvelles recherches sur la météorite de Cañon Diablo. *Comptes-rendus Académie des Sciences (Paris)*, 139, 773–780.
- (1905) Étude du siliciure de carbone de la météorite de Cañon Diablo. *Comptes-rendus Académie des Sciences (Paris)*, 140, 405–410.
- Moore, R.O., and Gurney, J.J. (1989) Mineral inclusions in diamond from the Monastery kimberlite, South Africa. In J. Ross, A.L. Jaques, J. Ferguson, D.H. Green, S.Y. O'Reilly, R.V. Danchin, and A.J.A. Janse, Eds., *Kimberlites and related rocks*, 2, p. 1029–1041. Blackwell Scientific, Cambridge, England.
- Navon, O., Hutcheon, I.D., Rossman, G.R., and Wasserburg, G.J. (1988) Mantle-derived fluids in diamond micro-inclusions. *Nature*, 335, 784–789.
- Ogbuji, L.U., Mitchell, T.E., Heuer, A.H., and Shinozaki, S. (1981) The  $\beta \rightarrow \alpha$  transformation in polycrystalline SiC: IV, A comparison of conventionally sintered, hot-pressed, reaction-sintered, and chemically vapor-deposited samples. *Journal of the American Ceramic Society*, 64, 100–105.
- Otter, M.L., and Gurney, J.J. (1989) Mineral inclusions in diamonds from the Sloan diatremes, Colorado-Wyoming State Line kimberlite district, North America. In J. Ross, A.L. Jaques, J. Ferguson, D.H. Green, S.Y. O'Reilly, R.V. Danchin, and A.J.A. Janse, Eds., *Kimberlites and related rocks*, 2, p. 1042–1053. Blackwell Scientific, Cambridge, England.
- Regis, A.J., and Sand, L.B. (1958) Natural cubic ( $\beta$ ) silicon carbide. *Geological Society of America Bulletin*, 69, 1633.
- Sato, H., and Shinozaki, S. (1974) Microsyntaxy and polytypism in SiC. *Material Research Bulletin*, 9, 679–684.
- Shinozaki, S., and Kinsman, K.R. (1978) Aspects of 'one-dimensional disorder' in silicon carbide. *Acta Metallogica*, 26, 769–776.
- Taylor, A., and Laidler, D.S. (1950) The formation and crystal structure of silicon carbide. *British Journal of Applied Physics*, 1, 174–181.
- Thibault, W.N. (1944) Morphological and structural crystallography and optical properties of silicon carbide (SiC). *American Mineralogist*, 29, 249–278, 327–362.
- Verma, A.R., and Krishna, P. (1966) Polymorphism and polytypism in crystals. Wiley, New York.
- Woermann, E., and Rosenhauer, M. (1985) Fluid phases and the redox state of the Earth's mantle. *Fortschritte der Mineralogie*, 63, 263–349.
- Zhang, P., and Chen, D. (1978) *Methods in diamond exploration*. Geological Publishing House, Beijing (in Chinese).

MANUSCRIPT RECEIVED JANUARY 20, 1989

MANUSCRIPT ACCEPTED AUGUST 10, 1990